Calcium Depletion Blocks the Maturation of Rotavirus by Altering the Oligomerization of Virus-encoded Proteins in the ER

Marianne S. Poruchynsky, David R. Maass, and Paul H. Atkinson

Department of Developmental Biology and Cancer, Albert Einstein College of Medicine, Bronx, New York 10461

Abstract. Maturation of rotavirus occurs in the ER. The virus transiently acquires an ER-derived membrane surrounding the virus particle before the eventual formation of double-shelled particles. The maturation process includes the retention and selective loss of specific viral protein(s) as well as the ER-derived membrane during formation of the outer capsid of the mature virus. When infected cells were depleted of Ca^{++} by use of the ionophore A23187 in calcium-free medium, membrane-enveloped intermediates were seen to accumulate. When Mn^{++}, an efficient Ca^{++} competitor, was used to replace Ca^{++} in the medium, the accumulation of the enveloped intermediate was again observed, pointing to an absolute requirement of Ca^{++} in the maturation process. It was previously demonstrated in this laboratory that a hetero-oligomeric complex of NS28, VP7, and VP4 exists which may participate in the budding of the single-shelled particle into the ER (Maass, D. R., and P. H. Atkinson. 1990. *J. Virol.* 64:2632-2641). The present study demonstrates that either in the absence of Ca^{++} or in the presence of tunicamycin, a glycosylation inhibitor, VP7 is excluded from these hetero-oligomers. In the presence of Mn^{++}, VP4 was blocked in forming a hetero-oligomeric complex with NS28 and VP7. The electrophoretic mobility of the viral glycoproteins synthesized in the presence of the ionophore were found to be altered. This size difference was attributed to altered N-linked glycosylation and carbohydrate processing of the viral glycoproteins. These results imply a major role for calcium and the state of glycosylation of NS28 in the assembly and acquisition of specific viral protein conformations necessary for the correct association of proteins during virus maturation in the ER.

ROTAVIRUS, a double capsid virus whose maturation process involves the ER (1, 7, 8, 10, 24), has provided a unique system in which to examine the posttranslational processing, targeting, and ER retention of both its nonstructural and structural glycoproteins, NS28 and VP7, respectively. Other studies have investigated the role of calcium in virus assembly (18, 22, 23), in the association of proteins within the ER (20), in the perturbation of egress of secretory proteins (13), and in the retention of soluble ER-targeted proteins to this organelle (6). It appears that the presence of cations and glycosylation plays a significant role in the association of proteins, possibly through conformational, energetic, or, in the case of the presence of cations, enzymatic mechanisms.

During maturation, rotavirus cores form in the viroplasm and acquire the inner capsid proteins to form single-shelled particles. NS28 is a transmembrane glycoprotein (2, 5) that modifies the ER and is the receptor for the subsequent budding of these single-shelled particles into the ER (3, 15) as the transient membrane-enveloped particle is formed. This intermediate membrane-enveloped particle has been isolated (16a) and comprises, in addition to the structural proteins of the virus, the nonstructural protein NS28. During virus maturation in the ER lumen, the membrane envelope is lost, giving rise to mature virus with VP7 and VP4 forming the outer capsid. In a previous study we show that VP4, VP7, and NS28 form a complex either before or during this maturation process (14). The role of calcium in rotavirus maturation has been studied by others (22), where budding of virus in cells maintained in calcium-free medium appeared to be inhibited (23). In the present study, when we used the calcium ionophore A23187 and EGTA to deplete the large calcium stores present in the ER (20), we observed, instead, that maturation appeared to be blocked after budding at the transient membrane-enveloped stage of virus. We have observed that in the presence of the ionophore, immature membrane-enveloped virus intermediates are formed exclusively, accumulate within the lumen of the ER, and do not uncoat. It was also determined that disruption of the hetero-oligomer complex occurred either in the presence of the ionophore or tunicamycin, a N-linked glycosylation inhibitor. Thus, the process by which there is selective retention of viral structural outer capsid proteins on the virus and the specific loss of the transmembrane nonstructural glycoprotein NS28, as

Dr. Marianne S. Poruchynsky's present address is Department of Molecular and Structural Biology, Ontario Cancer Institute, The Princess Margaret Hospital, 500 Sherbourne Street, Toronto, Ontario M4X 1K9 Canada.

well as other membrane elements, is perturbed under these conditions.

The morphological observations, taken together with the results from the biochemical cross-linking experiments presented in this study, suggest a role for calcium and glycosylation in the viral uncoating process and in the hetero-oligomerization of the rotavirus proteins VP4, VP7, and NS28 in the ER.

Materials and Methods

Cells and Virus

The fetal rhesus monkey kidney cell line, MA104, was grown as a monolayer in DME supplemented with 100 U of penicillin and 100 μg of streptomycin per ml, 2 mM-glutamine, 5% FCS, and 5% calf serum, (all from GIBCO Laboratories, Grand Island, NY) as described previously (9). Simian rotavirus SA11 was propagated at low multiplicity of infection in MA104 cells, isolated on cesium chloride gradients, and purified by the procedure of Street et al (25).

Infection of Cells and Ionophore Treatment

Confluent monolayers of MA104 grown on 35- or 100-mm dishes were infected at 20–30 pfu/cell, after trypsin activation of the inoculum, as described previously (9). Virus was allowed to adsorb to cells for 1–2 h at 37°C. The inoculum was removed, cells were rinsed in TBS, and those to be treated with the ionophore A23187 (Calbiochem Behring Corp., San Diego, CA) were either incubated in complete medium for 1–2 h or in DME salts lacking calcium, buffered with MOPS, Hepes, and *N*-Tris-(hydroxymethyl)-methyl-2-amino ethane sulphonic acid (TES), pH 7.6, containing all amino acids, 2 mM EGTA, and either 0.25, 1, 5, 10, or 25 μM of ionophore A23187, immediately after infection and for varying lengths of time ranging from 2 to 4 1/2 h. The ionophore was dissolved in DMSO and aliquots were diluted in sterile distilled water and sonicated immediately before addition to media. Before radiolabeling with Trans ^{35}S label (^{35}S-methionine and ^{35}S-cysteine) (ICN Biochemicals, Cleveland, OH), cells were incubated in calcium and methionine-free medium plus ionophore for 10 min, and then in the same medium lacking any methionine, but containing 100 μCi/ml Trans ^{35}S label for 1 h at 37°C. For the calcium replacement experiments, the calcium-free medium containing ionophore was replaced with buffered DME containing all amino acids and 1 mM $CaCl_2$ for the designated time, followed by incubation in methionine-depleted medium for 10 min before radiolabeling for 1 h in the presence of calcium. Control infected cells were incubated after virus adsorption in complete buffered medium containing all amino acids and 1 mM $CaCl_2$ until the labeling period began, at 4–4 1/2 h postinfection, at which time cells underwent the same 10-min prerinse and 1-h incubation in media with radiolabel as described. For the experiments examining short-term exposure to ionophore in the absence of calcium or for the pulse chases, 0.1–10 μM A23187 was added to cells 4 h after infection for a given length of time (0–20 min), cells then underwent a 5-min incubation in the same medium lacking methionine, and were then radiolabeled with Tran ^{35}S label for 5 min. Some samples were chased in medium without ionophore, containing 1 mM $CaCl_2$ and excess methionine, for times ranging from 5 to 90 min. Infected cells were also incubated 2 h p.i. either in the presence or absence of ionophore and calcium in medium containing 1.8 mM $MnCl_2$ for 2 h, and then radiolabeled with Tran ^{35}S label in the same medium for 1 h.

Endo-β-N-acetylglucosaminidase-H Treatment and PAGE

Infected radiolabeled cells had the labeling media removed and were rinsed with PBS at 4°C. The cells were scraped from the plates into PBS, pelleted, and resuspended in a lysis buffer containing 1% Triton X100 (TX100), 1% deoxycholate in 0.15 M NaCl, 0.025 M Tris, pH 8.0, 0.1% SDS, and Aprotinin (100 U/ml final concentration), vortexed, and had NP-40 and additional deoxycholate added, each to a final concentration of 0.5%. For the studies using Endo H (a gift from R. Trimble, New York State Department of Health, Albany, NY), duplicate aliquots of lysate had 1% SDS 0.05 M Tris, pH 6.7, and the buffer 0.2 M citrate phosphate, pH 5.0, added, the latter to a final molarity of 0.05. Samples were boiled for 3 min before the addition of 2.2 mU of Endo H. All samples, both untreated and treated, were incubated at 37°C for 1 h before aliquots were analyzed by 10% SDS-PAGE after the addition of 2× gel sample buffer containing DTT, PMSF, and other protease inhibitors, and boiling for 4 min. Gels were fixed in methanol/acetic acid and then fluorographed in Amplify (Amersham Corp., Arlington Heights, IL) before drying and exposure to Kodak SB5 film.

Crosslinking and Sucrose Gradient Sedimentation

After infection, monolayers were incubated in complete media for 2 h and then in calcium-free medium containing either 1 or 5 μM A23187 for an additional 2 h, before a short incubation in the same medium minus methionine and radiolabeling with Tran ^{35}S label for 1 h. Semi-intact cells were prepared as described (4, 14). Briefly, after the labeling period, monolayers were washed twice in 90 mM KCl, 50 mM Hepes, pH 7.5, then three times in 15 mM KCl, 10 mM Hepes, pH 7.5. Cells were allowed to swell by incubation in this buffer on ice, then scraped with a rubber policeman into 1.5 ml of 90 mM KCl, 50 mM Hepes, pH 7.5. Cells were pelleted at 2,000 rpm for 5 min at 4°C and resuspended in 500 μl of the same buffer. Chemical crosslinking was performed using the water-insoluble, thiol-cleavable, homobifunctional crosslinker, dithiobis(succinimidyl proprionate) (DSP; Pierce Chemical Co., Rockford, IL). A freshly prepared 50 mg/ml solution of DSP in DMSO was added to the semi-intact cell suspensions at a final concentration of 1.0 mg/ml (with DMSO concentration at 2%), which were then incubated at 22°C for 60 min. The reactions were terminated by the addition of 2 mM glycine to each and the cells were solubilized by the addition of Triton X100 and centrifuged on 5–20% sucrose gradients made up in 20 mM MOPS, 100 mM NaCl, 30 mM Tris, pH 7.5, containing 0.1% TX100, in an SW41 rotor at 37,000 rpm (175,000 *g*) at 4°C. The run was terminated at $\omega^2 t$ 0.9 × 10^{12} rad^2/s (18.5 h). The bottom of each tube was punctured with a 19-gauge needle and 22 drop fractions were collected (~1 ml). For each sample, 35-μl aliquots of each of the 12 fractions had gel 2× sample preparation buffer added containing protease inhibitors and DTT, were boiled, and analyzed by SDS-PAGE on 10% acrylamide gels.

For cells that were incubated in media containing manganese ions and whose proteins were crosslinked, cells were incubated in complete media for 3 h, and then in media containing 1.8 mM $CaCl_2$ with or without added 1.8 mM $MnCl_2$ for 1 h before a short incubation in the same medium minus methionine and radiolabeling with Tran ^{35}S label for 1 h. Semi-intact cells were prepared as described above and the proteins chemically crosslinked with DSP as described. After crosslinking, cells were lysed in a buffer appropriate for immunoprecipitation under denaturing conditions, and crosslinked hetero-oligomeric complexes were immunoprecipitated using the antibody to NS28. Immunoprecipitated crosslinked samples were reduced with DTT before gel electrophoresis.

Immunoprecipitation

Fractions from the gradients were divided into two equal volumes and then an equal volume of 2× lysis buffer was added. Immunoprecipitation was as described previously (14). After vortexing of the sample, NP-40 and deoxycholate were added to 0.5%, followed by the addition of SDS, to 2.0%. Samples were boiled for 4 min at 100°C and immunoprecipitation buffer A (9) was added as well as additional TX100. Samples were preincubated in preswollen protein A–Sepharose CL4B beads (Pharmacia Fine Chemicals, Piscataway, NJ) for 1–2 h at 4°C and then the beads were discarded. Each fraction had either 9 μl of rabbit anti-NS28-lac Z fusion protein (kindly provided by J. Rothblatt, Department of Biochemistry, University of California, Berkeley) or 7 μl of rabbit VP7 polyclonal antisera added. The VP7 antiserum was raised in a rotavirus-free rabbit, kept in germ-free isolation, against VP7 purified from an SDS polyacrylamide gel. The rabbit was a generous gift from M. Estes (Baylor University, Houston, TX). Samples were incubated with agitation at 4°C overnight followed by the addition of preswollen protein A–Sepharose CL4B beads and incubation for 3 h at 4°C. The beads were pelleted from the samples, washed twice in buffer B (0.15 M NaCl, 0.01 M Tris HCl, pH 8.3, 0.1% TX100, 0.005 M EDTA, and 100 Units/ml Aprotinin) and once in PBS. The protein antibody conjugates were dissociated from the protein A–Sepharose by boiling in 2× gel sample preparation buffer containing protease inhibitors and 50 mM DTT and were applied to 10% polyacrylamide gels.

Tunicamycin Treatment

SA11-infected MA104 cells, as described above, were treated with 2 μg/ml tunicamycin (Sigma Chemical Co., St. Louis, MO) for 4 h before labeling. Infected cells were radiolabeled with 100 μCi/ml Tran ^{35}S label in the presence of 2 μg/ml tunicamycin for 1 h at 37°C. Lysates were prepared, cross-

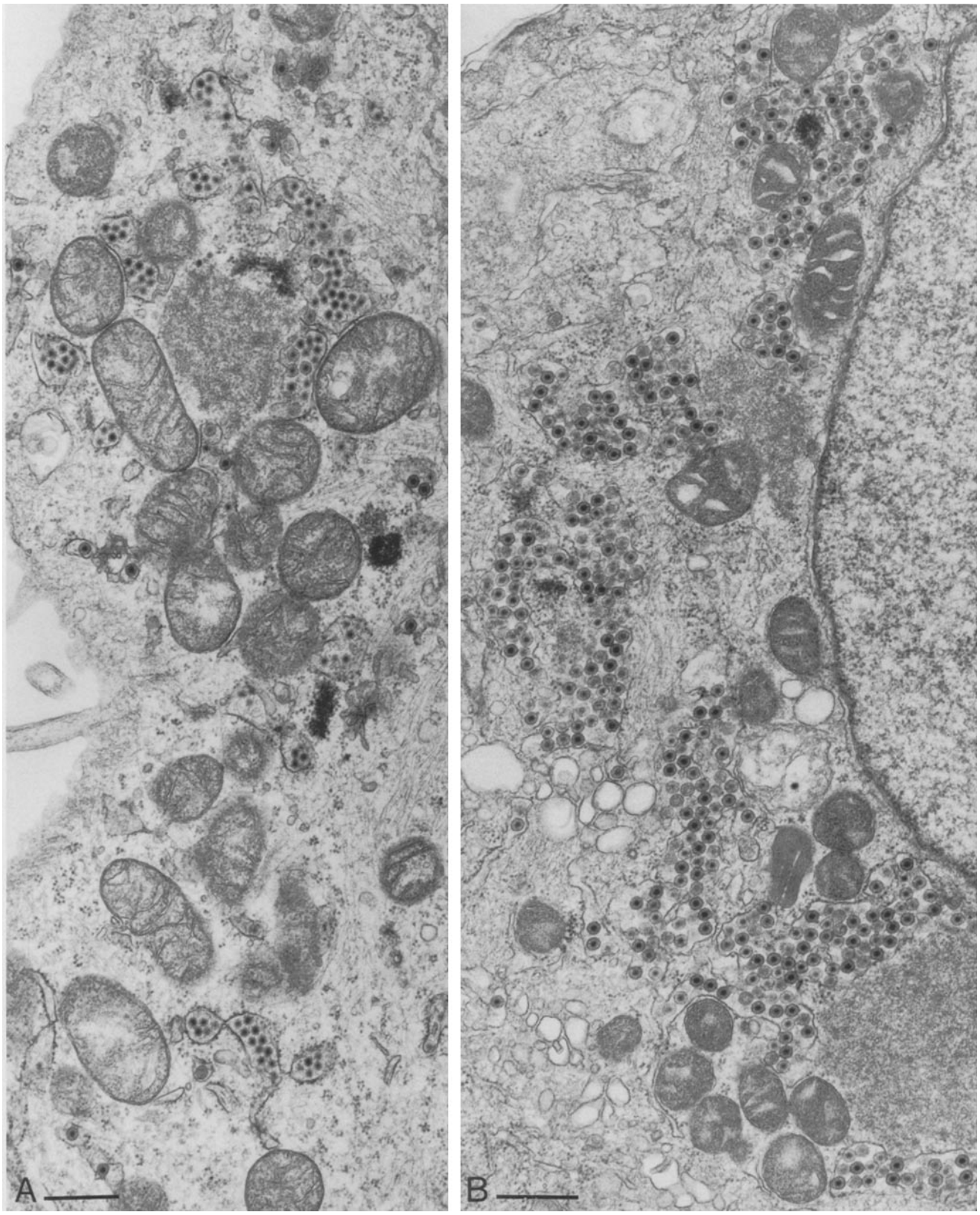

Figure 1. Comparison at low magnification, 5 h p.i. for each, of rotavirus SA11-infected MA104 cells incubated in medium containing the normal (1.8 mM) calcium concentration (*A*) and cells that were infected and then incubated in 1 μM of the ionophore A23187 in calcium-free medium for 4 h (*B*). Bars: (*A* and *B*) 500 nm.

linked with DSP, as described above, fractionated on sucrose gradients, and immunoprecipitated in the denatured state as described previously (14) and above.

EM

Infected cells that were incubated under ionic and ionophore conditions which were equivalent to those described for the radiolabeled cells, were fixed and embedded for EM. Cells incubated in either control or calcium-free medium containing the ionophore A23187 and EGTA for the particular interval, those which underwent calcium replacement after ionophore removal, or those that had the calcium in the medium replaced with manganese, each had their medium removed and were rinsed in PBS before their fixation at 22°C in 2% glutaraldehyde in 0.2 M cacodylate buffer for 45 min. The monolayers were embedded in epon, thin sectioned, and viewed in a JEOL 1200 electron microscope at 80 kV.

Results

Ultrastructural Morphology of Ionophore-treated SA11-infected Cells

The effect of calcium depletion on virus morphogenesis was examined in infected cells that were incubated in medium lacking calcium, and containing 2 mM EGTA and various concentrations of the calcium ionophore A23187.

Control cells in which the infection has been allowed to proceed for 4–5 h in the presence of calcium and the absence of ionophore, exhibit mostly mature viral forms within the ER and relatively few of the membrane-enveloped forms (Fig. 1 *A*). When cells in which the infection was allowed to proceed for 1 h after virus adsorption were then incubated in 1 μm A23187 for an additional 4 h and examined by thin section EM, viral single-shelled particles were visible at the periphery of cytoplasmic viroplasm structures alongside adjacent ER (Figs. 1 *B* and 2). Some of these cores were apparently in the process of budding into the ER (Fig. 2) or the nuclear envelope, an extension of the ER, thus acquiring a portion of the ER membrane and its associated proteins and becoming membrane encapsidated as they do so (Figs. 1 *B*, 2). The membrane-enveloped form, normally a transient intermediate, is the only form of virus seen to accumulate within the lumen of the ER, in many instances distending the normally compact ER luminal space (Figs. 1 *B*, and 2). No mature nonenveloped virus is ever visible within the ER lumen in the presence of any concentration of ionophore that was tested; 0.25, 1, 5, 10, or 25 μM. In ionophore-treated cells, virus core particles were sometimes seen aggregated in large numbers at the edge of a viroplasm structure and it appeared in some cases that elements of the ER were not present alongside the viroplasm (although this was not confirmed by serial thin-sectioning), and that ER membrane and its associated proteins were thus unavailable to accommodate these particles for budding (not shown). It has been suggested that the overall structure of the ER is altered and that fragmentation occurs when the calcium levels of cells are perturbed (11). The presence of the ionophore and the absence of calcium may have an effect on components of the ER membrane, such as the virus transmembrane glycoprotein NS28, which has been shown by in vitro studies to be essential for the binding of viral single-shelled particles to the ER via the inner capsid protein VP6 (2, 3, 15).

SA11-infected cells were also examined ultrastructurally to determine if the effect of calcium depletion was reversible. When cells were incubated in 0.25 μM ionophore for 2 h followed by a 2-h incubation in the absence of ionophore and the presence of 1.8 mM calcium, it was observed that all of the virus that had accumulated in the ER was still in the membrane-enveloped intermediate form and none had apparently matured correctly to the nonenveloped form (Fig. 3). There were, however, some virus forms whose membranes appeared broken or disrupted (Fig. 3, *arrowheads*). These forms did not appear to be identical to mature nonenveloped virus of infected control cells incubated in the presence of calcium and the absence of ionophore, which showed a distinctive spiked outer surface, probably composed of the outer capsid proteins (Fig. 3, *inset*, *arrows*). It may be that a new round of viral protein synthesis and virus

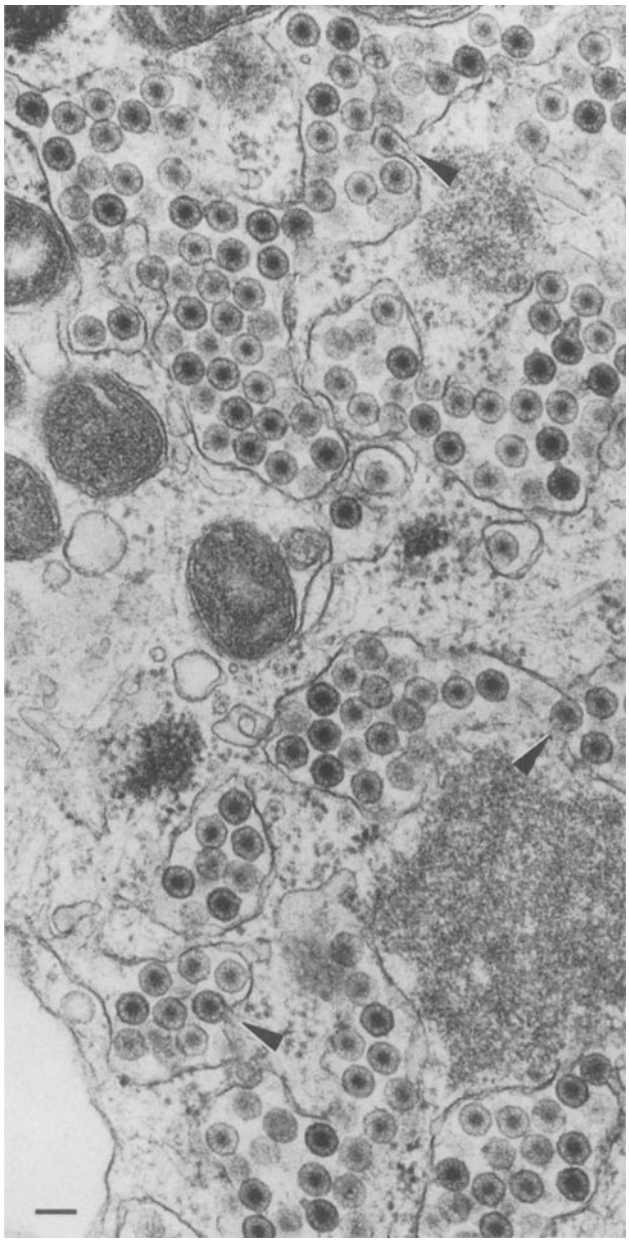

Figure 2. Higher magnification of a rotavirus-infected cell incubated in 1 μM A23187 in calcium-free medium for 4 h. Virus is seen budding into the ER (*arrowheads*) and the ER is distended with exclusively membrane-enveloped virus. Bar, 100 nm.

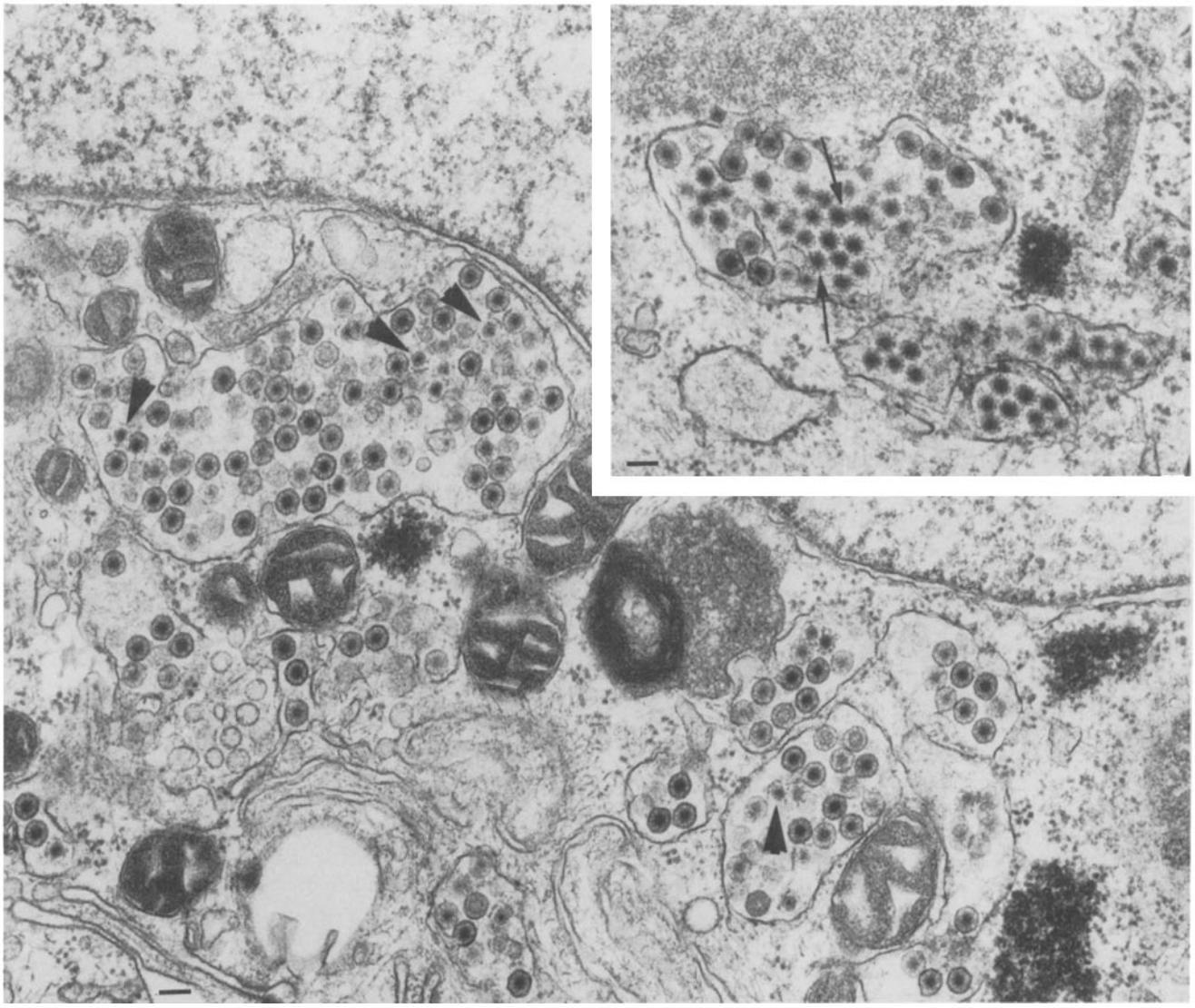

Figure 3. Comparison of rotavirus-infected control cells, with cells that were ionophore treated without calcium and then followed by calcium replacement in the absence of ionophore. At 2 h p.i., cells were incubated in 0.25 μM A23187 for 2 h, followed by a 2-h incubation in the absence of ionophore and the presence of 1.8 mM calcium. The control cells were infected and incubated in the presence of the normal (1.8 mM) concentration of calcium for 5 h p.i. (*inset*). Arrowheads denote disrupted virus. Inset, arrows denote normal, mature, nonenveloped double capsid virus. Bars, 100 nm.

formation in the absence of any residual effects of either the ionophore and/or the lack of calcium, is necessary in order to produce virus that has the ability to uncoat properly, or it may be that other cellular elements critical to the uncoating process have not recovered despite the presence of calcium and the removal of the ionophore.

There was no observed effect on virus maturation in Ca^{++}-free medium in the absence of ionophore (Fig. 4 *A*). However, when Mn^{++} replaced Ca^{++} in the medium, an arrest of virus at the enveloped particle stage of the maturation process was again observed, even in the absence of ionophore (Fig. 4 *B*).

Effect of Calcium Depletion on Viral Protein Synthesis

To assess the effect of the absence of calcium in the medium and the depletion of intracellular calcium stores on the synthesis and processing of the viral proteins, SA11-infected cells were incubated in the presence of various concentrations of the ionophore A23187 (0.25–25 μM). Generally, there was a progressive decrease in synthesis of all viral proteins as the concentration of the ionophore increased above 25 μm (data not shown). At low concentrations (0.25–1.0 μM), all rotavirus-encoded proteins appeared to be synthesized in stoichiometries and in amounts similar to controls (Fig. 5 *B*). The presence of ionophore in the absence of calcium in the medium also affected the glycosylation of VP7 and NS28. NS28 was observed as two distinct bands, corresponding to NS28 which was glycosylated at both positions, and at one position (Fig. 5, *A* and *B*). At higher ionophore concentrations (>5 μM), unglycosylated NS28 was also observed (Fig. 5 *A*). In ionophore-treated cells, it was observed that the two glycosylated forms of NS28 had a

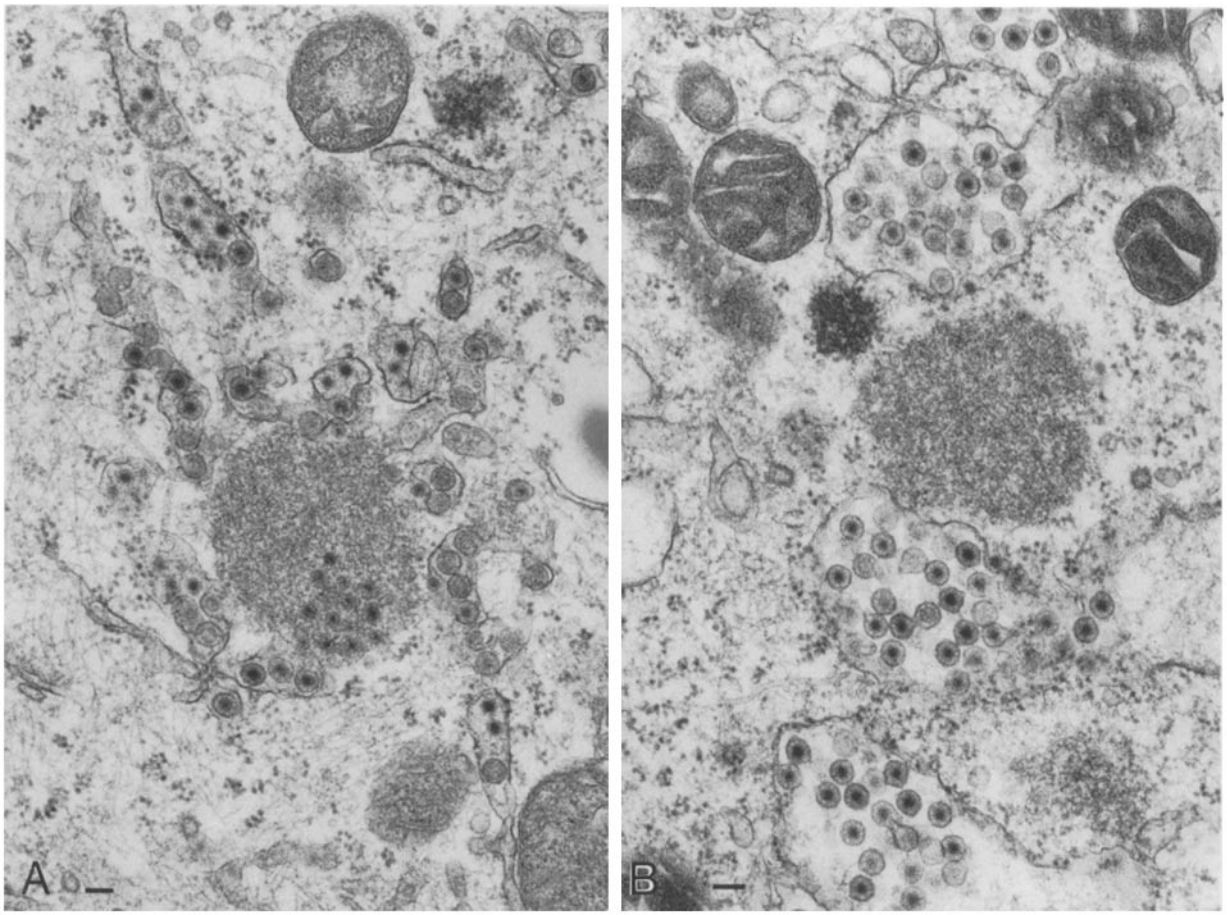

Figure 4. Comparison of rotavirus-infected cells, 5 h p.i., incubated in calcium-free medium in the absence of ionophore, either in the absence or presence of 1.8 mM $MnCl_2$ for the last 2.5 h of infection. Bars: (*A* and *B*) 100 nm.

faster electrophoretic mobility than the corresponding glycosylated forms of NS28 in the control (Fig. 5, *A* and *B*). VP7 also showed an alteration in its electrophoretic mobility, in that a more slowly migrating species was observed in addition to VP7 in the normal position (Fig. 5 *A*). VP7 and NS28 each showed a high-mannose, or ER form, of glycosylation in the presence of ionophore, as determined by their susceptibility to endo-β-N-acetylglucosaminidase-H (Endo H). VP7 and NS28 synthesized in the presence of the ionophore, and digested with Endo H, each comigrated with the totally deglycosylated forms of the two glycoproteins which are seen in the control (Fig. 5 *B*, *asterisks*). The ionophore effects on NS28 and VP7 glycosylation are likely due to changes in processing of the oligosaccharide and are not likely to involve incomplete lipid-oligosaccharide assembly, because although ionophore markedly alters NS28 processing it does not significantly alter VP7 processing (manuscript in preparation). When the ionophore was removed and the calcium depletion was reversed, the amount of processing of NS28 radiolabeled during the last hour of incubation, approximated that of the control and comigrated at the same position (Fig. 5 *B*). The presence of 2 mM EGTA in the medium, together with calcium in the absence of ionophore, had no apparent effect on virus morphology or on the pattern of the radiolabeled proteins (Fig. 5 *A*), when compared with the control. When the glucose concentration was increased from the normal 1 to 4 mg/ml in calcium-free medium containing 1 μM ionophore for 30 min before and during the 1-h labeling period, no change was observed in the nature or efficiency of glycosylation of NS28 (not shown). Therefore, it appears that the ionophore is not exerting its effects on glycosylation via an energy-dependent process that can be alleviated with added glucose.

Calcium depletion by the effects of the ionophore in calcium-free medium, exerted its maximum effects of both incomplete glycosylation of NS28 and more complete processing in ~20 min (Fig. 6, lanes *1–4*). To determine the time dependency of reversing depletion, a pulse-chase experiment was performed, where cells underwent a preincubation for 10 min in 2.5 μM ionophore, a 5-min prerinse in the same medium minus methionine, and a 5-min label, all in the presence of ionophore, followed by chase intervals in medium containing calcium and no ionophore. This pulse-chase regimen revealed that the depletion actually has two independent effects on glycosylation. Specifically, these include both the inhibition of glycosylation and the more complete processing of the oligosaccharides of NS28. This is revealed in the 5- and 15-min chases, where initially there appeared almost complete glycosylation of the two sites and NS28 appeared to be processed to the same extent as that of the control. By 30 min of chase, the faster migrating, more processed form characteristic of the calcium deprivation effect appeared.

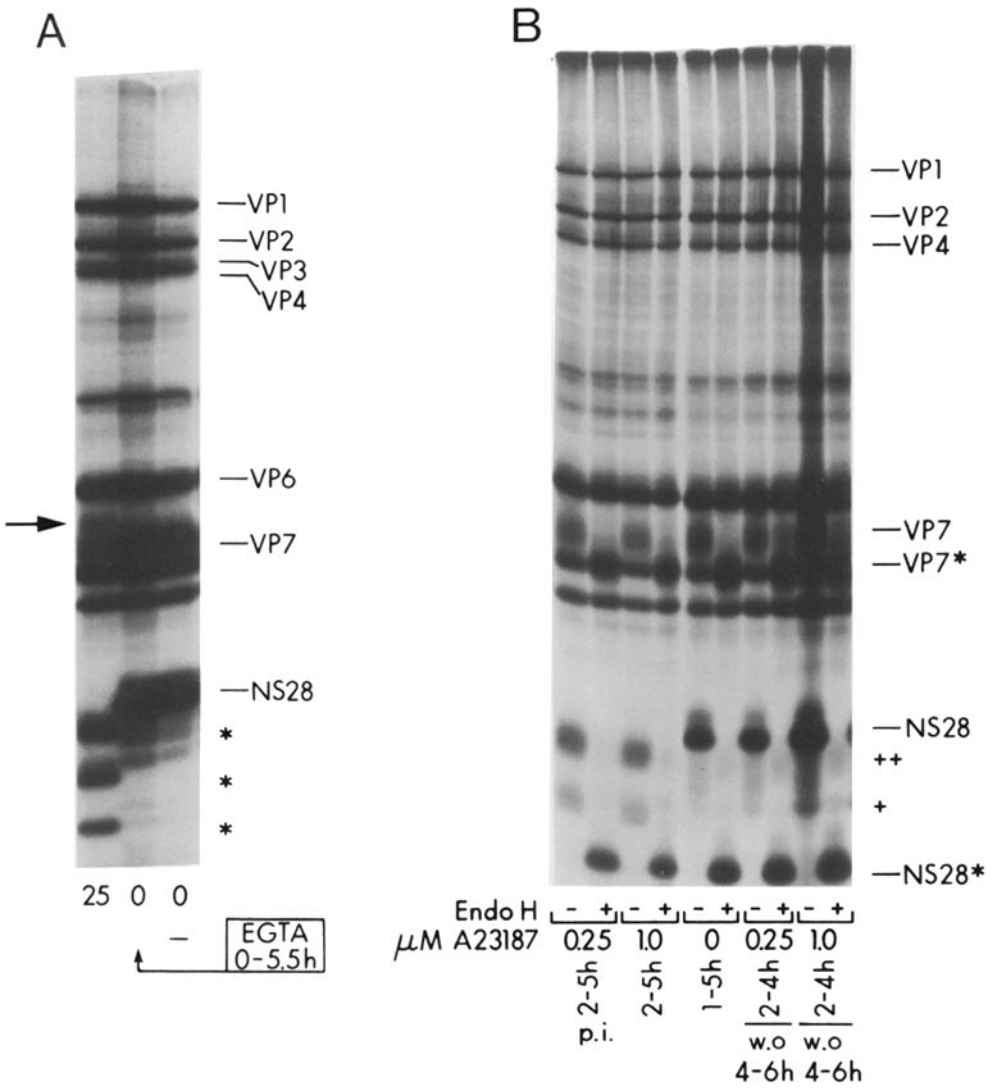

Figure 5. (*A*) Polyacrylamide gel analysis of rotavirus proteins in infected cells incubated in no ionophore (0 μM), in no ionophore (0 μM) plus EGTA for 5.5 h at 0 p.i. or a high concentration (25 μM) of ionophore A23187 in calcium-free medium and EGTA for 2.5 h at 3 h p.i. The arrow denotes the more slowly migrating form of VP7 and the asterisks denote the three altered positions of NS28, that glycosylated in two sites, one site, or not at all. (*B*) Endo-H digestion of rotavirus proteins in cells incubated in either 0.25 or 1.0 μM ionophore beginning 2 h p.i. for 3 h, or for 2 h and then followed by a 2-h incubation in medium containing calcium and lacking the ionophore. The asterisks denote the positions of both VP7 and NS28 after digestion with Endo H. The ++ and + denote the position of NS28 in its fully glycosylated (both sites) and partially glycosylated (one site) state.

Since Mn^{++} was shown to have a marked effect on virus maturation, its effect on VP7 and NS28 processing in the absence of calcium was examined as well. Mn^{++}, in the presence or absence of ionophore, resulted in exclusively relatively unprocessed VP7 (Fig. 7, *arrow*), but resulted in the same kind of increased processing of NS28 elicited by the ionophore (Fig. 7, *arrow*). Since the effect of the Mn^{++} on rotavirus glycoprotein processing was opposite in VP7 and NS28, it is unlikely the effects were due to a Ca^{++} requirement for the oligosaccharide processing glucosidases or α-mannosidases. It would seem that Ca^{++} is needed to maintain NS28 in a state that is incompatible for processing, whereas Ca^{++} appears to be necessary to maintain VP7 in a state in which it can be processed.

The Effect of Calcium Depletion on the Crosslinking of Viral Proteins

It has been shown by sucrose gradient velocity sedimentation of radiolabeled infected cells, that NS28 and VP7 can spontaneously oligomerize separately to form higher order structures (14) corresponding to dimers, trimers and tetramers. In the current study we repeated the observation and VP7 monomers (Fig. 8) peak in fractions 10 and 11, dimers in fractions 8 and 9, trimers in 7 and 8, and tetramers in 5 and 6 (14). This phenomenon could also be observed when cells were treated with 1 μM ionophore in the absence of calcium for 3 h (including the 1-h labeling period) (Fig. 8 *B*), where the pattern of distribution of all of the proteins across the gradient, including the additional partially glycosylated forms of NS28, is almost identical to that in the presence of calcium.

After treatment of infected radiolabeled cells with the thiol-cleavable crosslinker, DSP, and analysis of samples by sucrose gradient velocity sedimentation, it is observed that these oligomeric forms can be increased in infected cells (data not shown) as was shown previously (14). Higher order structures of NS28 and VP7 appeared which sedimented further into the gradient, and this was also observed for cells which were treated with 5 μM ionophore in the absence of calcium (data not shown).

To analyze the formation of hetero-oligomers of NS28, VP4 and VP7, each fraction of the sucrose gradient of material derived from infected cells that were treated or not

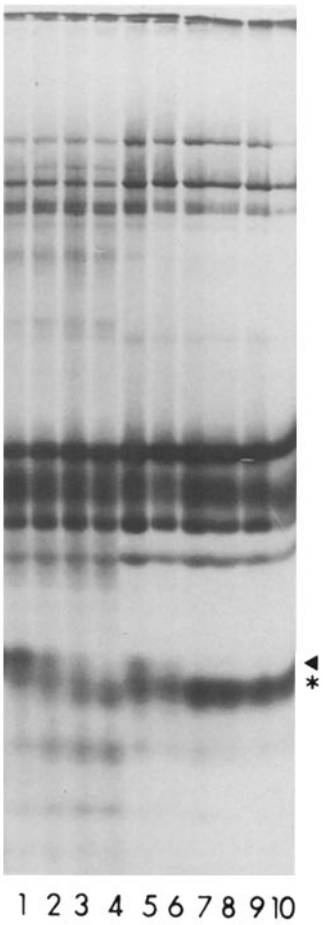

Figure 6. The effect of length of time of incubation in ionophore, on the glycosylation of NS28. Infected cells were incubated in 2.5 μM ionophore A23187 for 0, 5, 10, or 20 min (lanes 1–4, respectively), or for a fixed length of time, 10 min (lanes *5–10*), each followed by a 5-min preincubation in methionine-free medium containing ionophore and a 5-min labeling period in the same medium containing Tran ^{35}S-label. For the samples that underwent a chase, samples were incubated also in medium containing 1.8 mM $CaCl_2$ and without ionophore, for 5, 15, 30, 45, 60, or 90 min (lanes *5–10*, respectively). The arrowhead marks the normal position of completely glycosylated NS28 and the asterisk marks the more processed form of the oligosaccharides.

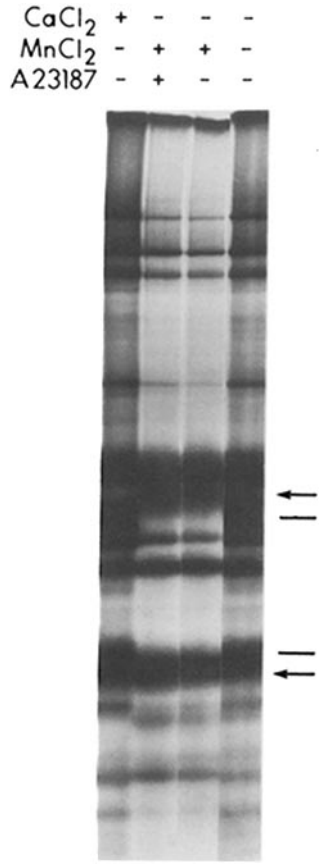

Figure 7. Polyacrylamide gel analysis of the effect of manganese on rotavirus proteins. Infected cells were incubated in medium lacking EGTA and calcium, containing 1.8 mM manganese, either in the presence or absence of ionophore for 2 h, and then radiolabeled for 45 min in Tran ^{35}S label and compared with cells infected in the presence of normal calcium levels and labeled for 2.25 h. Bars denote the normal positions of NS28 and VP7; arrows, the altered positions of the two glycoproteins.

treated with ionophore and crosslinked with DSP, was immunoprecipitated with a polyclonal antibody to NS28 and then reduced. NS28, reduction-resistant dimers of NS28, VP4, and VP7 were observed as part of a crosslinked complex (Fig. 9 *A*), and it was noted that the peak in abundance of these molecules occurred in the same fraction. However, when the fractions derived from infected cells treated with 5 μM ionophore were immunoprecipitated in the same manner, NS28 with all of its glycosylation forms was precipitated across the gradient, as was the reduction-resistant NS28 dimer and even VP4, but VP7 was conspicuously absent from this complex in these cells (Fig. 9 *B*). When duplicate aliquots of these fractions were immunoprecipitated with a polyclonal antibody to VP7, one observes that VP7 is present across the gradient, but peaks in abundance in a much lighter fraction, showing an ability to form dimers of VP7 (14) but not hetero-oligomers (Fig. 9 *C*). Thus, NS28-VP4 is unable to complex with VP7 in the ionophore-treated cells. When cells were treated with 2 μg/ml tunicamycin for 5 h and the proteins crosslinked and separated on gradients (data not shown), identical results were obtained, showing an inability of VP7 to complex with NS28-VP4. Mn^{++}, an efficient Ca^{++} competitor, blocked the ability of VP4 to participate in the hetero-oligomerization of NS28, VP7, and VP4, which occurs under normal conditions where Ca^{++} is present as the only cation (Fig. 10).

These results collectively show the importance of calcium ions in the normal hetero-oligomerization of virus proteins and the resultant maturation of rotavirus particles.

Discussion

The results presented in this paper demonstrate an essential role for Ca^{++} in the assembly and maturation of rotavirus components within the ER. The precise mechanism is not clear, but the following observations taken together are pertinent. First, in the absence of Ca^{++}, maturation of virus from the membrane-enveloped intermediate to the nonenveloped form is blocked. In addition, α-mannosidase processing of NS28 is enhanced and that of VP7 is inhibited. Although a rabbit liver α-mannosidase has been shown to be a calcium ion–requiring enzyme (21), the mannosidase that is acting on NS28 is present in infected cells, and apparently does not have an absolute requirement for Ca^{++}. Oligosaccharide analysis of the carbohydrates on NS28 by HPLC, derived from cells treated with ionophore in the absence of calcium, shows that increased mannosidase processing of the carbohydrate has occurred (manuscript in preparation). In the presence of Mn^{++}, maturation is again arrested at the enveloped viral intermediate and the processing of NS28 is again more extensive than that of controls. It has been noted in the literature, that treatment of infected cells with tunicamycin, an inhibitor of N-linked glycosylation, results in the production of only membrane-enveloped particles (16, 19). These observations implicate a role for glycosylation in the assembly of rotavirus outer shell proteins and the maturation

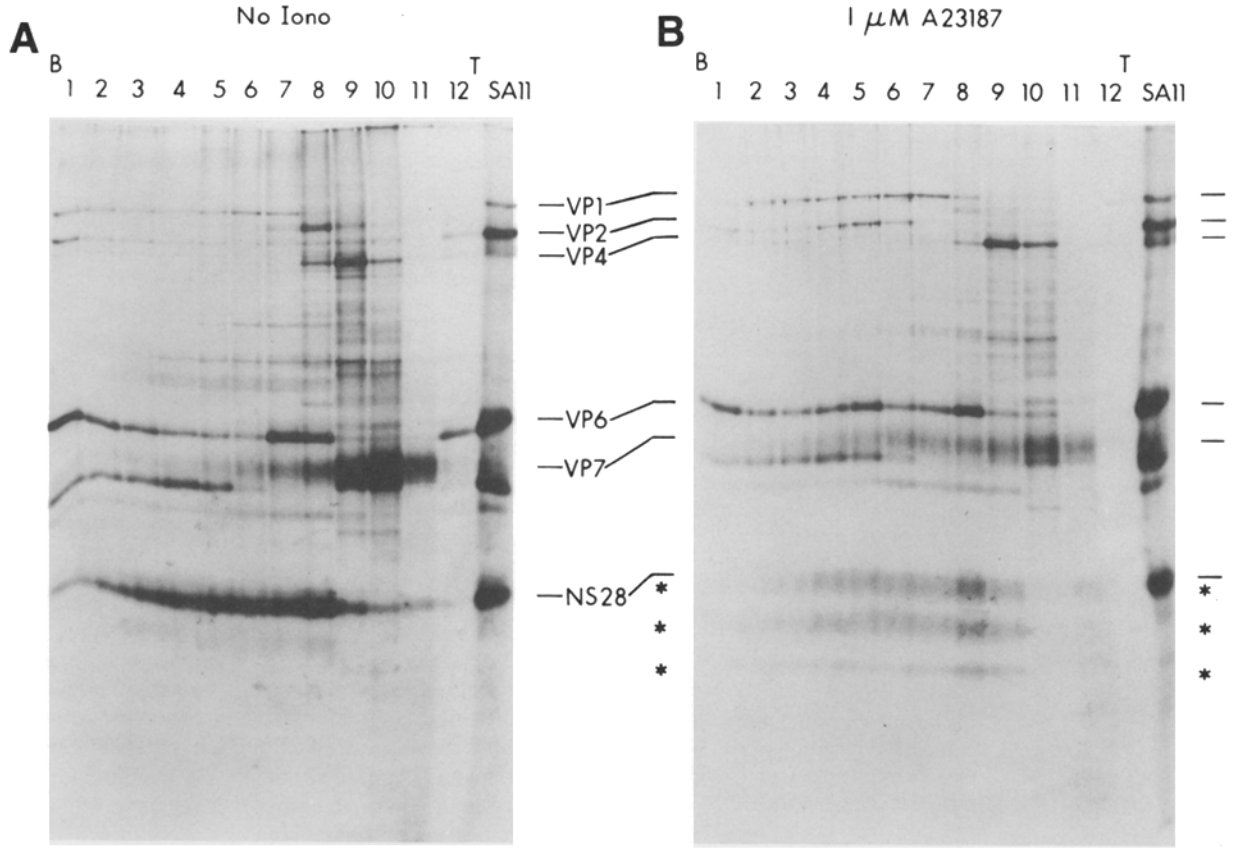

Figure 8. (*A* and *B*). The effect of the ionophore A23187 and the absence of calcium on the oligomerization of viral proteins. Lysates of rotavirus-infected cells were incubated in calcium-free medium containing either no ionophore or 1 μM ionophore for 2 h before a 1-h labeling period in the same media containing Tran ^{35}S label. Lysate samples were centrifuged on 5–20% linear sucrose gradients in 90 mM KCl, 50 mM Hepes, pH 7.5, containing 0.1% TX100, 175,000 *g* for 18.5 h. Aliquots of fractions of complexed material were reduced with DTT before application to the gel. B and T denote the bottom and top of the gradient, respectively. The virus proteins are labeled and asterisks denote the more rapidly migrating, partially, and unglycosylated forms of NS28. SA11 denotes the complete radiolabeled infected cell lysate as a marker lane and the two gels represent equivalent amounts of cellular material. Viral proteins seen at the top of the gradient arise from the pellet as the last fraction exits at the bottom of the gradient.

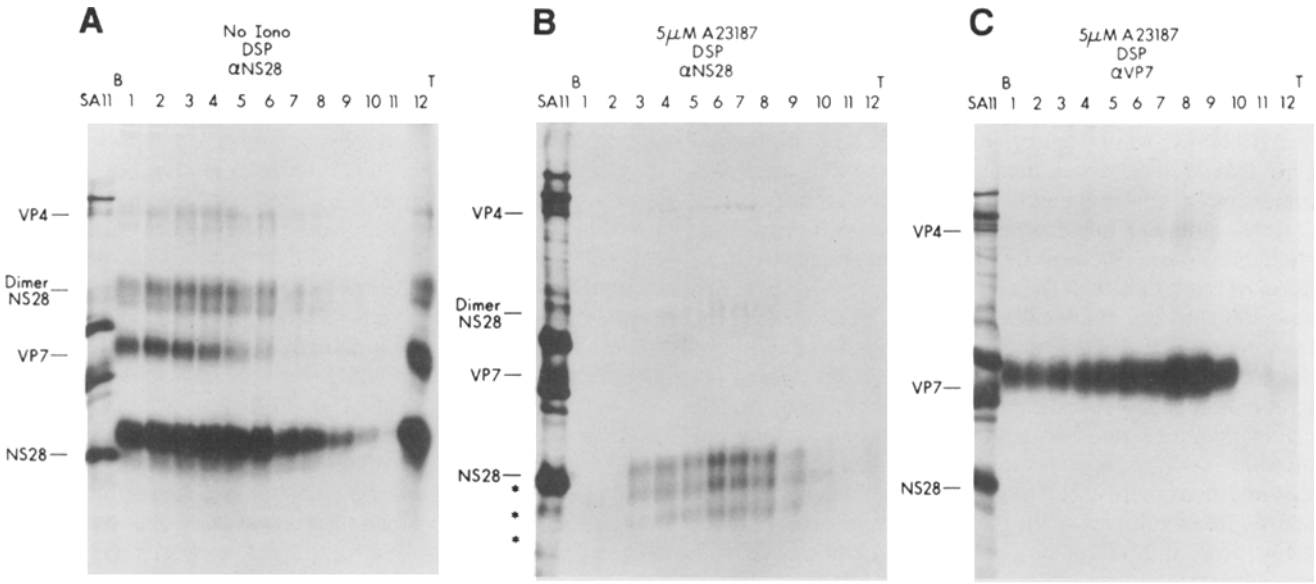

Figure 9. Immunoprecipitation of DSP crosslinked viral protein complexes from 5–20% sucrose gradient fractions using either polyclonal antisera to NS28-lac Z fusion protein (*A* and *B*) or to VP7 (*C*). The fractions were derived from infected cell lysates that were either treated with 5 μM ionophore, or not, and were reduced with DTT before electrophoresis. Viral proteins are indicated, as is the reduction-resistant dimer of NS28. B and T denote the bottom and top of the gradient, respectively. The asterisks denote the more rapidly migrating, partially, and unglycosylated forms of NS28. In *B*, the first two fractions had only half of the sample loaded onto the gel.

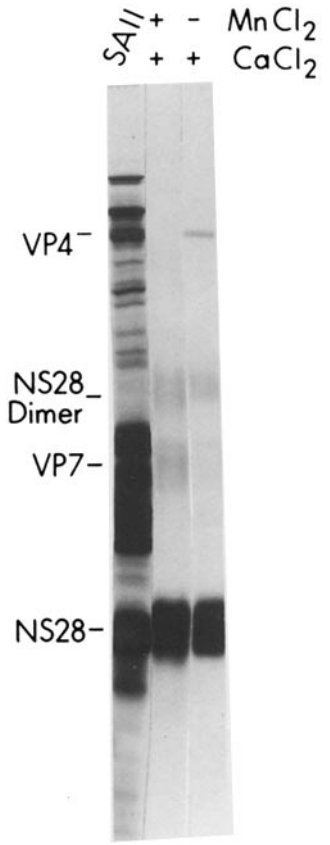

Figure 10. Crosslinked proteins after incubation in medium containing calcium alone or both calcium and manganese, followed by immunoprecipitation with anti-NS28. Infected cells, 3 h p.i., were incubated in medium containing 1.8 mM $CaCl_2$, with or without added 1.8 mM $MnCl_2$ for 1 h before labeling for 1 h in Tran ^{35}S-label. The proteins of semi-intact cells were crosslinked with DSP as described in Materials and Methods, lysed, and then immunoprecipitated with anti-NS28. The immunoprecipitated crosslinked complexes were reduced with DTT before SDS-PAGE.

of virus from the membrane-enveloped intermediate form. A variant of rotavirus has been described which naturally lacks the single glycosylation site on VP7 and whose NS28 is glycosylated normally. Cells infected with the variant exhibited normal, mature, nonenveloped infectious virus production (16), implying that the glycosylation of NS28, and not necessarily VP7, may be crucial for the association of various proteins and the correct events of the maturation process to occur. Two possible interpretations of the glycosylation state of NS28 during virus maturation are feasible. The first is a direct involvement of normal NS28 high mannose carbohydrate in a lectin-like interaction with other rotavirus proteins, in particular VP7. The second possibility is that in the absence or alteration of NS28 glycosylation, specific conformations of viral proteins may not be attained, and, as a result, the normal process of virus maturation is unable to proceed. A possible explanation for the increased processing seen on NS28 in the absence of calcium and presence of ionophore is due to its association with membranes of ER and virus in a configuration that allows NS28 to remain accessible to carbohydrate-processing enzymes. It is also conceivable that there are energetic and enzymatic processes that require specific cations for the uncoating process, one possibility being that of a calcium-activated phospholipase. The result of the inability to form a cross-linked complex of the three virally encoded proteins, NS28, VP7, and VP4, was observed for cells treated with tunicamycin, and may be an indication of disrupted interactions between proteins. Whatever the immediate role of NS28 glycosylation, the crosslinking studies indicate a probable change in the conformation of the viral protein(s) in the absence of calcium and in the presence of the ionophore. This was reflected by the inability to crosslink the three proteins into a hetero-oligomeric complex that was immunoprecipitable with antibody to NS28 under these conditions, when compared to conditions of normal calcium concentration in the media, where the complex of three proteins was retrieved. This inability to immunoprecipitate the NS28, VP7, and VP4 as a complex, occurred in spite of the presence of substantial amounts of VP7, which retained the ability to form thiol-cleavable oligomers with itself. The precipitation of an NS28-VP7 complex, and the absence of VP4 when manganese ions were allowed to compete with calcium, implies a differential cationic requirement for the viral proteins as well.

It has been proposed that NS28 has potential sites for binding Ca^{++} (2), although actual cation binding by the protein has never been shown. The cessation of the formation of mature infectious virus at the membrane-enveloped step apparently was not reversible, since when the normal calcium levels were restored in the medium and the ionophore was absent for an incubation period of several hours, enveloped particles were still observed. This result implies either that the virus and/or the proteins themselves are in a configuration that cannot proceed to the next step in the maturation process, or that there are residual effects of the presence of the ionophore or the absence of calcium on other influential cellular mechanisms. Apparently the lack of calcium did not influence the retention of both of these viral glycoproteins to the ER, as the processing on both of these proteins remained sensitive to Endo H. This is of interest in light of recent discussion (6, 13) on the need for Ca^{++} for retention of some proteins in the ER. The ionic, enzymatic, and energetic requirements for protein associations and rearrangements, and the resultant maturation of rotavirus particles can be further explored by performing in vitro studies on the isolated transiently membrane-enveloped virus particles.

We thank J. Rothblatt and R. Trimble for their kind gifts of antibody and enzyme, respectively. The technical expertise of R. P. Kawakami and J. Lee, for the growth and propagation of SA11 rotavirus, is greatly appreciated.

This work was supported by Public Health Service grants R01-CA13402-17 and core cancer grant PO1-CA13330 from the National Institutes of Health.

Received for publication 15 January 1991 and in revised form 30 April 1991.

References

1. Altenburg, B. C., D. Y. Graham, and M. K. Estes. 1980. Ultrastructural study of rotavirus replication in cultured cells. *J. Gen. Virol.* 46:75–85.
2. Au, K.-S., W.-K. Chan, and M. K. Estes. 1989. Rotavirus morphogenesis involves an endoplasmic reticulum transmembrane glycoprotein. *In* Cell Biology of Viral Entry, Replication and Pathogenesis, New Series. R. Compans, A. Helenius, and M. Oldstone, editors. UCLA Symp. Mol. Cell. Biol. 1990. Alan R. Liss, Inc., New York. 257–267.
3. Au, K.-S., W.-K. Chan, J. W. Burns, and M. K. Estes. 1989. Receptor activity of rotavirus nonstructural glycoprotein NS28. *J. Virol.* 63:4553–4562.
4. Beckers, C. J. M., D. S. Keller, and W. E. Balch. 1987. Semi-intact cells permeable to macromolecules: use in reconstitution of protein transport from the endoplasmic reticulum to the Golgi complex. *Cell.* 50:523–534.
5. Bergmann, C. C., D. Maass, M. S. Poruchynsky, P. H. Atkinson, and A. R. Bellamy. 1989. Topology of the non-structural rotavirus receptor glycoprotein NS28 in the rough endoplasmic reticulum. *EMBO (Eur. Mol. Biol. Organ.) J.* 8:1695–1703.
6. Booth, C., and G. L. E. Koch. 1989. Perturbation of cellular calcium induces secretion of luminal ER proteins. *Cell.* 59:729–737.

7. Estes, M. K., E. L. Palmer, and J. F. Obijeski. 1983. Rotaviruses: a review. *Curr. Top. Microbiol. Immunol.* 105:123–184.
8. Holmes, I. H. 1983. Rotaviruses. *In* The Reoviridae. W. K. Joklik, editor. Plenum Publishing Corp., New York. 359–423.
9. Kabcenell, A. K., M. S. Poruchynsky, A. R. Bellamy, H. B. Greenberg, and P. H. Atkinson. 1988. Two forms of rotavirus VP7 are involved in assembly of SA11 rotavirus in endoplasmic reticulum. *J. Virol.* 62: 2929–2941.
10. Kapikian, A. Z., and R. M. Chanock. 1985. Rotaviruses. *In* Virology. B. N. Fields, editor. Raven Press, New York. 863–906.
11. Koch, G. L. E., C. Booth, and F. B. P. Wooding. 1988. Dissociation and reassembly of the endoplasmic reticulum in live cells. *J. Cell Sci.* 91:511–522.
12. Liu, M., P.A. Offit, and M. K. Estes. 1988. Identification of the simian rotavirus SA11 genome segment 3 product. *Virology.* 163:26–32.
13. Lodish, H. F., and N. Kong. 1990. Perturbation of cellular calcium blocks exit of secretory proteins from the rough endoplasmic reticulum. *J. Biol. Chem.* 265:10893–10899.
14. Maass, D. R., and P. H. Atkinson. 1990. Rotavirus proteins, VP7, NS28, and VP4 form oligomeric structures. *J. Virol.* 64:2632–2641.
15. Meyer, J. C., C. C. Bergmann, and A. R. Bellamy. 1989. Interaction of rotavirus cores with the nonstructural glycoprotein NS28. *Virology.* 171:98–107.
16. Petrie, B. L., M. K. Estes, and D. Y. Graham. 1983. Effects of tunicamycin on rotavirus morphogenesis and infectivity. *J. Virol.* 46:270–274.
16a. Poruchynsky, M. S., and P. H. Atkinson. 1991. Rotavirus protein rearrangements in purified membrane-enveloped intermediate particles. *J. Virol.* In press.
17. Ready, K. F. M., and M. Sabara. 1987. In vitro assembly of bovine rotavirus nucleocapsid protein. *Virology.* 157:189–198.
18. Ready, K. F. M., M. I. J. Sabara, and L. A. Babiuk. 1988. In vitro assembly of the outer capsid of bovine rotavirus is calcium dependent. *Virology.* 167:269–273.
19. Sabara, M., L. A. Babiuk, J. Gilchrist, and V. Misra. 1982. Effect of tunicamycin on rotavirus assembly and infectivity. *J. Virol.* 43:1082–1090.
20. Sambrook, J. F. 1990. The involvement of calcium in transport of secretory proteins from the endoplasmic reticulum. *Cell.* 61:197–199.
21. Shutzbach, J. S., and W. T. Forsee. 1990. Calcium ion activation of rabbit liver α1,2-mannosidase. *J. Biol. Chem.* 265:2546–2549.
22. Shahrabadi, M. S., and P. W. K. Lee. 1986. Bovine rotavirus maturation is a calcium-dependent process. *Virology.* 152:298–307.
23. Shahrabadi, M. S., L. A. Babiuk, and P. W. K. Lee. 1987. Further analysis of the role of calcium in rotavirus morphogenesis. *Virology.* 158:103–111.
24. Soler, C., C. Musalem, M. Lorono, and R. T. Espejo. 1982. Association of viral particles and viral proteins with membranes in SA11-infected cells. *J. Virol.* 44:983–992.
25. Street, J. E., M. C. Croxson, W. F. Chadderton, and A. R. Bellamy. 1982. Sequence diversity of human rotavirus strains investigated by Northern blot hybridization analysis. *J. Virol.* 43:369–378.